THE JOURNAL OF PHYSICAL CHEMISTRY B

Article

pubs.acs.org/JPCB

Interaction between Water and Alkali Metal Ions and Its Temperature Dependence Revealed by Oxygen K-Edge X-ray Absorption Spectroscopy

Masanari Nagasaka,*[,†,‡] Hayato Yuzawa,[†] and Nobuhiro Kosugi[†,‡]

[†]Institute for Molecular Science, Myodaiji, Okazaki 444-8585, Japan

[‡]SOKENDAI (Graduate University for Advanced Studies), Myodaiji, Okazaki 444-8585, Japan

ABSTRACT: Interaction between water molecules and alkali metal ions in aqueous salt solutions has been studied by the oxygen K-edge soft X-ray absorption spectroscopy (XAS) in transmission mode. In the measurement of several alkali halide aqueous solutions with different alkali chlorides (Li, Na, and K) and different sodium halides (Cl, Br, and I), the pre-edge component arising from the hydration water molecules shows a blue shift in peak energy as strongly depending on cations but not on anions. In the temperature dependent measurement, the pre-edge component arising from water molecules beyond the first hydration shell shows the same behavior as that of pure liquid water. On the other hand, the pre-edge component arising from water molecules in the first hydration shell of Li^+ ions is not evidently dependent on the temperature, indicating that the hydration water molecules are more strongly bound with Li^+ ions than the other water molecules. These experimental results are supported by the results of radial distribution functions of the first hydration shell and their temperature dependence, evaluated by molecular dynamics simulations.

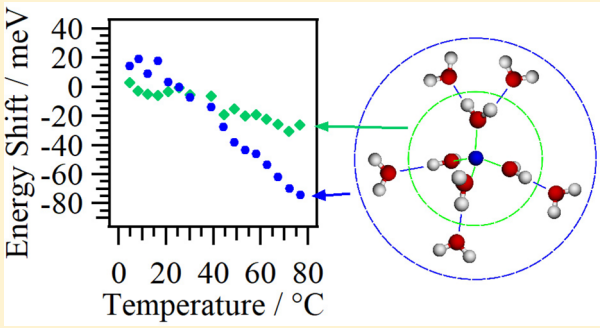

1. INTRODUCTION

Macroscopic properties of aqueous salt solutions, such as viscosity, boiling point, and freezing point, are influenced by the interaction between solute ions and solvent water molecules.[1−3] Recently, hydration structures of ions in aqueous salt solutions were extensively studied by neutron diffraction.[4−9] Ohtomo et al. studied hydration structures of Li^+ ions in LiCl solutions.[4] Mancinelli et al. studied hydration structures of Na^+ and K^+ ions in NaCl and KCl solutions.[8] Hydration structures of ions in aqueous salt solutions were also studied by X-ray scattering[10−13] and extended X-ray absorption fine structure.[14,15] Megyes et al. studied coordination numbers of Na^+ ions by X-ray diffraction.[16] The electronic structures of alkali halide aqueous solutions were studied by photoelectron spectroscopy[17] and X-ray emission spectroscopy.[18−20] Hydration structures of cations were also studied by molecular dynamic (MD) simulations.[21−34] Most of them focused on the coordination number and the distance of ions with hydrating water molecules.

In aqueous salt solutions, the cation is weakly bound to oxygen atoms of water molecules, whereas the anion is weakly bound to hydrogen atoms. Na K-edge X-ray absorption spectroscopy (XAS) revealed that both Na^+ and Cl^- ions share the same water molecules in highly concentrated NaCl solutions.[35] These solvent-shared ion pairs in LiCl solutions were also confirmed by dielectric relaxation spectroscopy.[36] The interaction of anions with water molecules was extensively studied by using the OH stretch vibration mode in Raman spectroscopy.[37−39] Smith et al. reported that the bond of anions with water molecules becomes weaker in the order of F^-, Cl^-, Br^-, and I^- ions.[39] On the other hand, the hydration shell of cations in aqueous salt solutions has not yet been studied in detail. This is because there are few effective methods to investigate the interaction of cations with water molecules.

The local structure of liquid water has been extensively studied by the O K-edge XAS.[40−52] The pre-edge peak (535 eV) of pure liquid water corresponds to a transition from O 1s to the $4a_1$ unoccupied orbital of water molecule, where the $4a_1$ orbital is mainly distributed on the oxygen atom of water molecule. Therefore, the pre-edge peak could be affected by the interaction of hydrating water molecules with cations. Several groups discussed the hydration structure of cations from the energy shift of the pre-edge peaks in O K-edge XAS of aqueous salt solutions by several detection techniques.[53−59] Näslund et al. measured O K-edge XAS of NaCl and KCl solutions in fluorescence yield,[53] and discussed that the spectral changes are caused by the interaction of cations with water molecules. On the other hand, Cappa et al. studied O K-edge XAS of aqueous salt solutions from total electron detection of liquid microjet,[54,55] and proposed that the spectral changes are caused by the electronic perturbation of water molecules by anions. Juurinen et al. measured O K-edge XAS of LiCl solutions at

Received: October 3, 2017
Revised: November 6, 2017
Published: November 13, 2017

DOI: 10.1021/acs.jpcb.7b09789
J. Phys. Chem. B 2017, 121, 10957−10964

different concentrations by using the hard X-ray Raman scattering, and observed that the pre-edge peak is shifted to the higher photon energy by increasing the concentration.[58] Waluyo et al. measured O K-edge XAS of aqueous salt solutions in transmission mode by using a droplet of liquid sample sandwiched between two Si_3N_4 membranes, and proposed that the pre-edge peaks are influenced by the hydration structures of cations.[57,59] Thus, the previous experimental results and discussion are inconsistent with each other. In order to solve the inconsistency, it is necessary to measure reliable O K-edge XAS of different aqueous salt solutions in transmission mode.[60]

In addition, the temperature dependence of O K-edge XAS spectra is also important in investigation of the hydration structure of cations in aqueous salt solutions. Several groups measured O K-edge XAS of liquid water at different temperatures.[43,44,47,49,51,52] They revealed that the pre-edge peak in XAS spectra reflects a local structural change of the hydrogen bond (HB) network at different temperatures. The temperature effect of liquid water has also been studied by neutron diffraction,[61] nuclear magnetic resonance,[62] X-ray Compton scattering,[63,64] infrared and Raman spectroscopy,[65−68] and MD simulations.[68−70] Waluyo et al. measured O K-edge XAS of aqueous salt solutions at different temperatures by using hard X-ray Raman scattering,[59] and observed the pre-edge peak shift dependent on the temperature. However, reliable XAS in transmission mode has not yet been reported from the viewpoint of temperature dependence of aqueous salt solutions.

We have been developing several kinds of liquid flow cells for XAS in transmission mode.[48,60,71,72] In the present work, we investigate the hydration structure in aqueous alkali halide solutions by O K-edge XAS in transmission mode. Especially, we have concentrated on the interaction between alkali metal ions and hydrating water molecules to select aqueous LiCl, NaCl, KCl, NaBr, and NaI solutions. From XAS spectra of different cations and anions, we confirm that the pre-edge peak shift is strongly dependent on cations but not on anions, and that the temperature dependence of O K-edge XAS spectra of LiCl solutions arises mainly from bulk water, beyond the first hydration shell of Li^+ ions. We perform MD simulations of some aqueous salt solutions to support the experimental investigation.

2. METHODS

2.1. XAS Measurements. We have carried out O K-edge XAS measurements at the soft X-ray undulator beamline BL3U at UVSOR-III Synchrotron.[73] Details of a transmission-type liquid flow cell used in the present work were described previously.[48,60,72] In the liquid flow cell, a liquid layer is sandwiched between two 100 nm thick Si_3N_4 membranes with the windows size of 2×2 mm^2 (NTT AT). Teflon spacers with the thickness of 100 μm are set between the support plates of the Si_3N_4 membranes. Liquid samples are exchangeable *in situ* by using a tubing pump. Temperature of a liquid sample is controllable from −5 to 80 °C. The liquid flow cell is in atmospheric helium condition, which is separated by a 100 nm thick Si_3N_4 membrane window from the soft X-ray beamline in ultrahigh vacuum condition. This windows size determines the soft X-ray beam size on the sample. In the present work, we have chosen 200×200 μm^2 for use of more photon fluxes though 30×30 μm^2 is possible to choose. Soft X-rays under vacuum pass through the membrane window, a liquid layer sandwiched by the two membranes in the helium buffer region, and finally a photodiode detector. The thickness of liquid sample layer is at most 2000 nm at the helium pressure of 0.1013 MPa in the helium buffer region. By increasing the helium pressure, the liquid sample layer becomes thinner to deform the two elastic membranes of the liquid sample, and the liquid thickness is at minimum 20 nm at the helium pressure of 0.12 MPa. The energy resolution of incident soft X-rays is set to 0.4 eV. XAS spectra are obtained by using Lambert−Beer law, $\ln(I_0/I)$, where I_0 and I are the transmission signal of blank and liquid sample, respectively. The photon energy is calibrated by the O 1s → π^* peak (530.80 eV) of O_2 gas mixed a little in the helium buffer gas.[74]

2.2. MD Simulations. In order to obtain radial distribution functions (RDF) of cations with hydrating water molecules, we have carried out MD simulations by using GROMACS 4.6.1.[75,76] The potentials of ions are described by OPLSAA,[77,78] and that of water molecule is described by TIP5P.[79] The temperature is controlled by the Nosé−Hoover thermostat method.[80,81] The pressure is adjusted by the Parrinello−Rahman method.[82] The simulation is performed at a time step of 1 fs with a periodic boundary condition and the partial-mesh Ewald method.[83] The unit cell consists of about 500 water molecules and several ions considering molar concentrations of aqueous salt solutions. Randomly distributed structures are optimized by the simulations, which run during 100 ps at 100 K in the NVT condition, 100 ps at 200 K and 1 atm in the NPT condition, and 2 ns at a destination temperature and 1 atm in the NPT condition. The equilibrium structures are obtained by sampling the structures every 1 ps during a simulation time of 20 ns.

3. RESULTS AND DISCUSSION

3.1. Dependence of Cation and Anion. Figure 1a shows O K-edge XAS spectra of liquid water and aqueous salt solutions with different cations (3 M LiCl, 3 M NaCl, and 3 M KCl) at 25 °C. The XAS spectrum of liquid water shows three well-known features: pre-edge peak (535 eV), main-edge maximum (537 eV), and post-edge maximum (540 eV). The intensities of the post-edge maximum of aqueous salt solutions are decreased as compared to that of pure liquid water, indicating that the HB network is partially broken by ions and the multiple scattering in the HB network is weakened. As shown in the inset of Figure 1a, the pre-edge peaks of aqueous salt solutions show higher energies (blue shifts) than that of pure liquid water. Different cations show different pre-edge peak energies, and the LiCl solution shows the largest blue shift of the three alkali chloride solutions. Figure 1b shows O K-edge XAS of liquid water and aqueous salt solutions with different anions (3 M NaCl, 3 M NaBr, and 3 M NaI) at 25 °C. The pre-edge peaks of NaCl are slightly higher in energy than those of NaBr and NaI solutions, but are rather smaller than those of LiCl. These results indicate that the energy shift of the pre-edge peaks is predominantly caused by the hydration structures of alkali metal ions. It is reasonable considering that the $4a_1$ orbital related to the pre-edge peak is mainly distributed on the oxygen atom of water.

Assuming that the water molecules beyond the first hydration shells of cations have almost the same HB networks as in pure bulk water, the pre-edge features can be decomposed into the contribution from the water molecules (O_{fw}) in the first hydration shells of cations and the contribution from the other water molecules (O_{bw}) beyond the first hydration shell. In Figure 2, the pre-edge peak in O K-edge XAS of 3 M LiCl

DOI: 10.1021/acs.jpcb.7b09789
J. Phys. Chem. B 2017, 121, 10957−10964

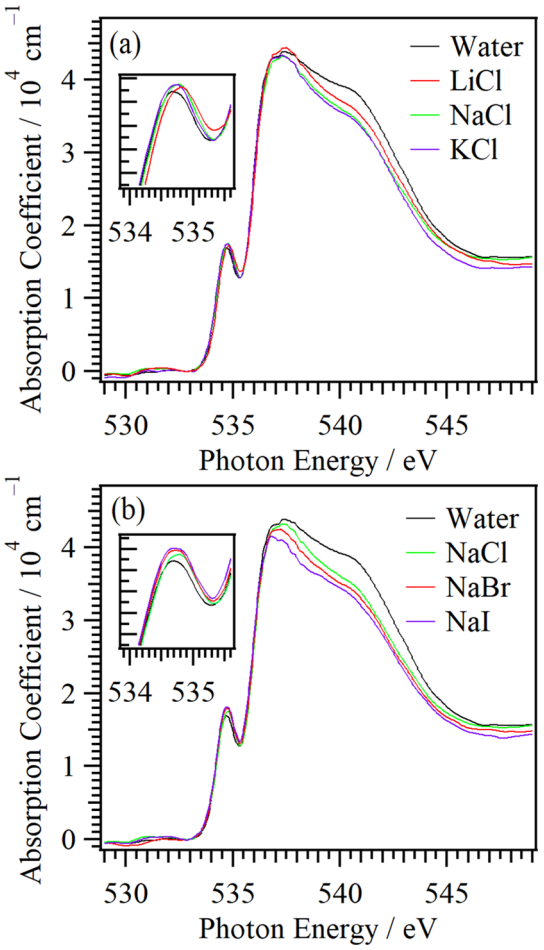

Figure 1. (a) O K-edge XAS spectra of pure liquid water and aqueous salt solutions with different cations (3 M LiCl, 3 M NaCl, and 3 M KCl) at 25 °C. (b) O K-edge XAS spectra of pure liquid water and aqueous salt solutions with different anions (3 M NaCl, 3 M NaBr, and 3 M NaI) at 25 °C. The insets show the expansions of the pre-edge regions.

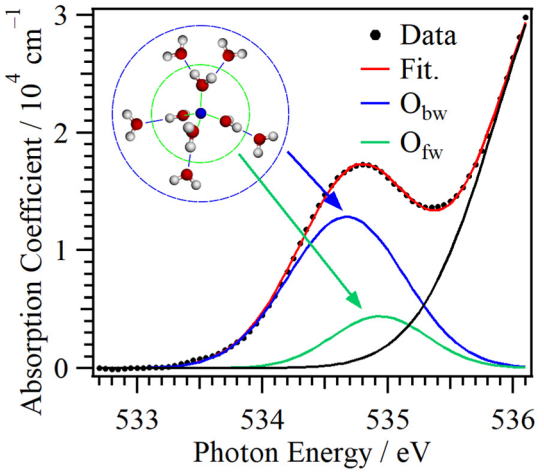

Figure 2. An example of the fitting of the pre-edge peak in O K-edge XAS of 3 M LiCl solution, assuming that the pre-edge feature consists of the hydrating water molecules (O_{fw}) in the first hydration shell of Li^+ ions and the other water molecules (O_{bw}). The intensity ratio is the same as the ratio of numbers of O_{fw} and O_{bw}. The black line is the fitted curve of the main-edge maximum (537 eV).

solution is fitted by assuming that the pre-edge peak arising from O_{bw} is the same as that of pure liquid water. In this fitting analysis, the number of O_{fw} is referred from the neutron diffraction studies:[4,8] 4 for Li^+, 5 for Na^+, and 6 for K^+ ions. The intensity ratio of bulk water is evaluated as 78% in 3 M LiCl solution, where the ratio of the number of ions and molecules, Li^+:O_{fw}:O_{bw} = 1:4:14. There are two major components in the O K-edge spectra, bulk water beyond the first hydration shell and water of the first hydration shell, directly interacting with the cation. The spectral contribution from bulk water (known) is subtracted in the fitting analysis considering the intensity ratios of O_{fw} and O_{bw}, and then the spectral contribution from hydration water can be obtained, though water of the second hydration shell may be slightly different from bulk water.

Table 1 shows the pre-edge peak energy of O_{fw} and the energy shifts ΔE of O_{fw} in comparison with pure liquid water at

Table 1. Pre-Edge Peak Energy of Hydrating Water Molecules (O_{fw}) in the First Hydration Shell of Cations at 25 °C Determined from the Results Shown in Figure 1 by the Fitting Shown in Figure 2, and the Energy Difference ΔE from the Pre-Edge Peak Energy of Pure Liquid Water

samples	energy (eV)	ΔE (eV)
pure liquid water	534.67	
5 M LiCl	534.97	0.30
3 M LiCl	534.94	0.27
3 M NaCl	534.76	0.09
3 M KCl	534.67	0.00
3 M NaBr	534.71	0.04
3 M NaI	534.69	0.02

25 °C. In alkali chlorides, the cation effect is remarkable: Li^+ (0.27 eV), Na^+ (0.09 eV), and K^+ (0.00 eV). Because the energy shift of Li^+ ion in 5 M LiCl solution (0.30 eV) is close to that in 3 M, the contribution of O_{fw} is successfully extracted in the present fitting procedures. On the other hand, in sodium halides, the anion effect is rather small: Cl^- (0.09 eV), Br^- (0.04 eV), and I^- (0.02 eV). Note that the energy shifts of pre-edge peak in different anions from pure water include the interaction of Na^+ ions with surrounding water molecules. In highly concentrated aqueous salt solutions above 1 M, it was reported that water molecules share both cations and anions and the electronic structure of water molecules in the first hydration shells of cations is also influenced by anions.[35] Even if so, the large energy shift of LiCl solutions indicates that the pre-edge peak energy arises predominantly from the interaction of cations with O_{fw}. Thus, the pre-edge peak shift indicates that the hydration of Li^+ ions is stronger than that of Na^+ ions, and that of Na^+ ions is stronger than that of K^+ ions.

In order to confirm the relation between the pre-edge peak shift and the interaction of cations with water molecules in the first hydration shell, we have evaluated RDF in different aqueous salt solutions by using MD simulations. Figure 3a shows RDF of cations (M^+) with oxygen atom of water molecules (O_w) in different aqueous salt solutions with the concentration of 3 M. The positions of the first peaks in RDF M^+-O_w of Li^+, Na^+, and K^+ ions are 1.99, 2.37, and 2.69 Å, respectively. These results are in good agreement with the neutron diffraction results,[4,8] showing that the bond lengths of Li^+, Na^+, and K^+ ions with O_w are 1.90, 2.34, and 2.65 Å, respectively. The coordination number of Li^+ ions obtained by MD simulation is around 4, and is also consistent with the

DOI: 10.1021/acs.jpcb.7b09789
J. Phys. Chem. B 2017, 121, 10957−10964

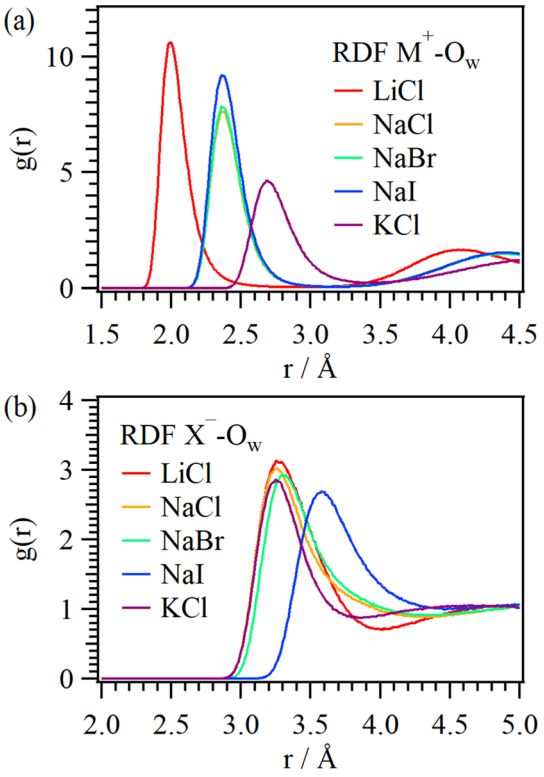

Figure 3. (a) RDF of cations (M^+) with oxygen atoms of water molecules (O_w) in different aqueous salt solutions with the concentration of 3 M. (b) RDF of anions (X^-) with O_w in different aqueous salt solutions.

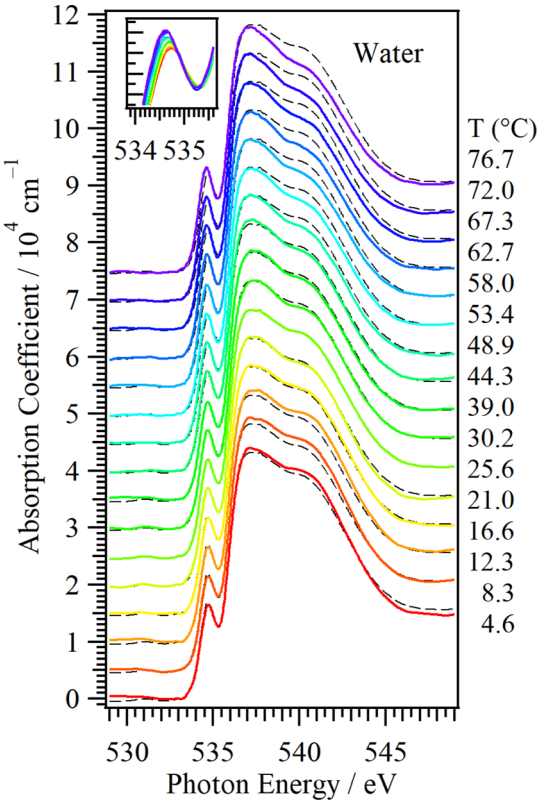

Figure 4. O K-edge XAS spectra of liquid water at different temperatures. The dashed lines show the reference spectrum at 25.6 °C. The inset shows the pre-edge region.

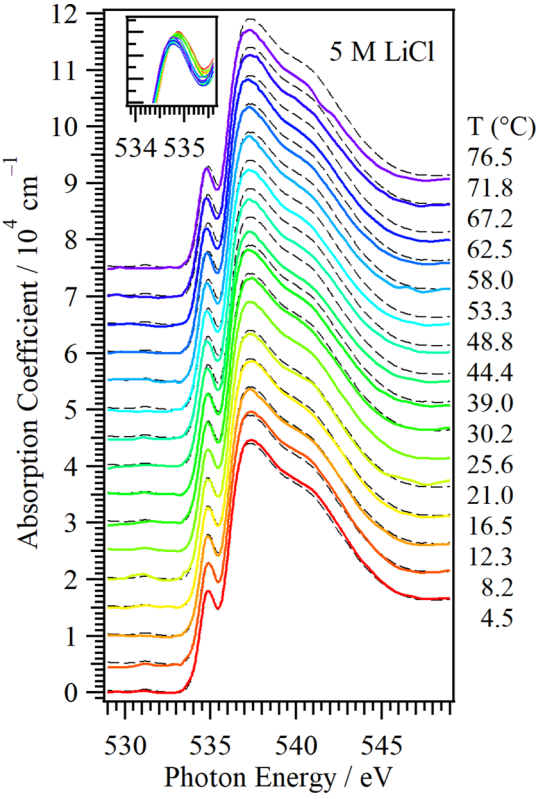

Figure 5. O K-edge XAS spectra of 5 M LiCl solutions at different temperatures. The dashed lines show the reference spectrum at 25.6 °C. The inset shows the pre-edge region.

neutron diffraction results.[4] The RDF M^+-O_w with different anions (NaCl, NaBr, and NaI) shows that the first peak of Na^+ ions are not changed irrespective of anions. Figure 3b shows RDF of anions (X^-) with O_w in aqueous salt solutions. The positions of the first peaks in RDF X^--O_w of Cl^-, Br^-, and I^- ions are 3.26, 3.30, and 3.58 Å, respectively, which are rather longer than those of cations; therefore, the interaction of anions with water molecules would be too small to show a noticeable pre-edge energy shift. This result is consistent with the experimental result.

3.2. Temperature Effects of Hydration Shells. In order to investigate the temperature dependence of the hydration shell in aqueous salt solutions, we have measured O K-edge XAS spectra of liquid water and 5 M LiCl solutions at different temperatures, as shown in Figures 4 and 5, respectively. In O K-edge XAS spectra of liquid water, the intensity of the post-edge maximum is decreased at the higher temperature, indicating that the HB network is partially broken at the higher temperature and the multiple scattering in the HB network is weakened. On the other hand, as shown in the inset of Figure 4, the pre-edge peak energy is lowered by increasing the temperature. Figure 6a shows the temperature dependence of the energy shift of the pre-edge peak from 25.6 °C in liquid water. The energy shift is −93 meV from 8.3 to 76.7 °C. This result is almost consistent with previously measured temperature dependence of O K-edge XAS spectra of liquid water by several detection techniques.[43,44,47,49,51,52] The smooth temperature dependence of the pre-edge peak energy arises from the temperature dependence of the HB distance (namely, volume expansion), because the longer HB distance reduces the exchange and electrostatic interactions between nearest

DOI: 10.1021/acs.jpcb.7b09789
J. Phys. Chem. B 2017, 121, 10957−10964

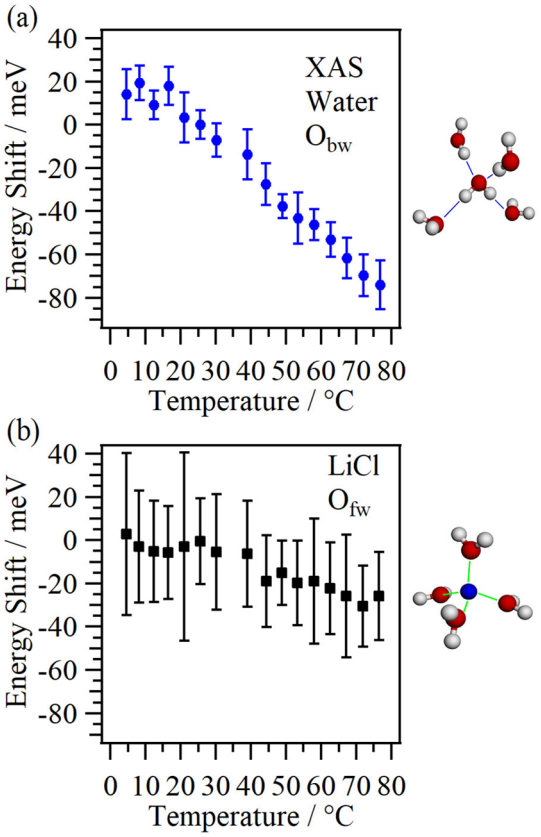

Figure 6. (a) Temperature dependence of the pre-edge peak energy in O K-edge XAS spectra of pure liquid water as compared with the reference spectrum at 25.6 °C. The inset shows a typical HB structure in liquid water. (b) Temperature dependence of the pre-edge peak energy of the hydrating water (O_{fw}) of Li^+ ions in 5 M LiCl solutions as compared with the reference spectrum at 25.6 °C. The inset shows a typical hydration structure of Li^+ ions.

neighbor water molecules, resulting in red shift of the pre-edge peak. Here, we do not have to consider the HB network breaking effect on the pre-edge peak shift.

Figure 5 shows O K-edge XAS spectra of 5 M LiCl solutions at different temperatures. The intensities of the post-edge maximum are decreased by increasing the temperature, indicating that the HB network is partially broken by ions. On the other hand, the pre-edge peak energy is lowered (red-shifted) at the higher temperature. The pre-edge features in 5 M LiCl solutions can be decomposed into the contributions from O_{fw} and O_{bw} by the same fitting procedure shown in Figure 2, where the bulk water components (O_{bw}) are obtained from XAS of pure liquid water at different temperatures shown in Figure 4. Figure 6b shows the pre-edge peak shift of O_{fw} in 5 M LiCl solution at different temperatures. The energy shift for O_{fw} is −23 meV from 8.2 to 76.5 °C, and is much smaller than that of bulk water (−93 meV). This result indicates that the hydration water molecules are more strongly bound with Li^+ ions than the other water molecules and show much smaller temperature dependence than the bulk water.

In order to investigate the temperature effect of the hydration shell of Li^+ ions theoretically, we have evaluated RDF in 5 M LiCl solutions at different temperatures by using MD simulations. Figure 7a shows RDF of Li^+ ions with oxygen atoms in water molecules (O_{fw}) in the first hydration shell at different temperatures. The peak position in RDF Li^+-O_{fw} is 2.00 Å at 5 °C, and is slightly shorten by increasing the temperature (1.98 Å at 80 °C). The hydration shells of Li^+ ions are slightly pressed by the elongation of HB network of water at higher temperatures. This result is consistent with the previous MD simulations,[24] where the first peaks in RDF Li^+-O_w are not changed at different temperatures. Figure 7b shows RDF of O_{fw} with oxygen atoms of water molecules (O_{bw}) beyond the first hydration shell at different temperatures in 5 M LiCl solutions. The first peak position in RDF O_{fw}-O_{bw} becomes longer with increasing the temperature, in which the distances are 2.71 Å at 5 °C and 2.76 Å at 80 °C. Figure 7c shows RDF O_{bw}-O_{bw} at different temperatures in 5 M LiCl solutions. The first peak position in RDF O_{bw}-O_{bw} in 5 M LiCl aqueous solutions is 2.71 Å at 5 °C and 2.76 Å at 80 °C, the same as RDF O_{fw}-O_{bw}. As shown in Figure 7d, RDF O_{bw}-O_{bw} in pure liquid water at different temperatures are also 2.71 Å at 5 °C and 2.76 Å at 80 °C, the same as RDF O_{fw}-O_{bw} and RDF O_{bw}-O_{bw} in 5 M LiCl aqueous solutions. The MD results are consistent with the present O K-edge XAS results, indicating that the interaction of Li^+ ions with hydrating water molecules (O_{fw}) is stronger than the HB network beyond the first hydration shell and is much less dependent on the temperature. In addition, the MD results indicate clearly that the HB interaction beyond the first hydration shell is the same as that of pure liquid water.

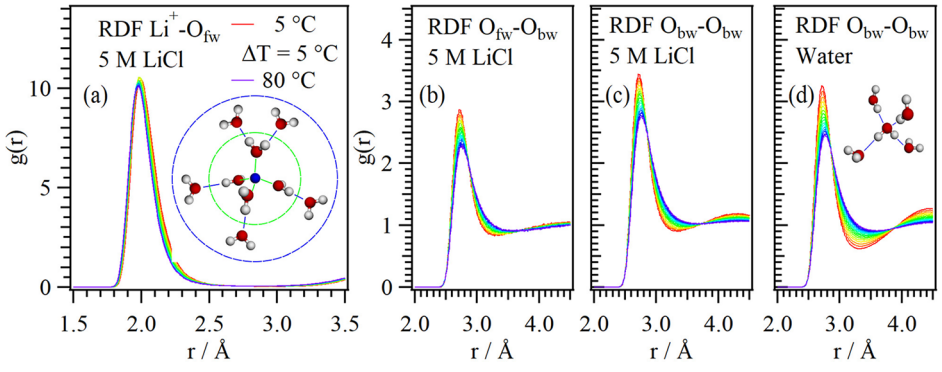

Figure 7. (a) RDF of Li^+ ions with oxygen atoms of hydrating water molecules (O_{fw}) in the first hydration shell in 5 M LiCl aqueous solutions as a function of temperature in the order of rainbow color. The inset shows the first hydration shell of Li^+ ions and water molecules (O_{bw}) beyond the first hydration shell. (b) RDF of O_{fw} with O_{bw} in 5 M LiCl solution as a function of temperature. (c) RDF O_{bw}-O_{bw} in 5 M LiCl solution as a function of temperature. (d) RDF O_{bw}-O_{bw} in pure liquid water as a function of temperature. The inset shows a typical HB structure in pure liquid water.

DOI: 10.1021/acs.jpcb.7b09789
J. Phys. Chem. B 2017, 121, 10957−10964

4. CONCLUSIONS

We have investigated the hydration effect of alkali metal cations in aqueous salt solutions on the pre-edge peak of O K-edge XAS in transmission mode for various aqueous salt solutions with different cations (LiCl, NaCl, and KCl) and anions (NaCl, NaBr, and NaI). Due to the interaction of cations with water molecules in the first hydration shell, the pre-edge peak is shifted to the higher energy (blue shift) in comparison with pure liquid water, in the order of K^+, Na^+, and Li^+ ions, which mean that the hydration strength is in the order of Li^+, Na^+, and K^+ ions. We have performed the temperature dependent XAS measurements of pure liquid water and 5 M LiCl solutions. Assuming that the number of water molecules in the first hydration shell is 4 and the pre-edge component of the other water molecules, beyond the first hydration shell, shows the same temperature dependence as of bulk water, the spectral decomposition results show that the pre-edge component of water molecules in the first hydration shell is not evidently dependent on the temperature. It indicates that the interaction of Li^+ ions with hydrating water molecules is strong enough to keep the first hydration shell of Li^+ ions irrespective of the temperature. This experimental result is in good agreement with the result of MD simulations.

AUTHOR INFORMATION

Corresponding Author

*E-mail: nagasaka@ims.ac.jp.

ORCID

Masanari Nagasaka: 0000-0002-6249-6553

Notes

The authors declare no competing financial interest.

ACKNOWLEDGMENTS

This work is supported by JSPS Grants-in-Aid for Scientific Research (JSPS KAKENHI Grant Nos. 20350014, 23245007, 23685006, 26248010, and 17H03013), Grant for Basic Science Research Projects from the Sumitomo Foundation, and Morino Foundation for Molecular Science. The authors acknowledged Mr. Toshio Horigome for his contribution to the development of the liquid flow cell and the staff members of UVSOR-III Synchrotron for their kind support. The computations were performed using Research Center for Computational Science, Okazaki, Japan.

REFERENCES

(1) Ohtaki, H.; Radnai, T. Structure and Dynamics of Hydrated Ions. *Chem. Rev.* **1993**, *93*, 1157−1204.

(2) Jenkins, H. D. B.; Marcus, Y. Viscosity *B*-Coefficients of Ions in Solution. *Chem. Rev.* **1995**, *95*, 2695−2724.

(3) Marcus, Y. Effect of Ions on the Structure of Water: Structure Making and Breaking. *Chem. Rev.* **2009**, *109*, 1346−1370.

(4) Ohtomo, N.; Arakawa, K. Neutron Diffraction Study of Aqueous Ionic Solutions. I. Aqueous Solutions of Lithium Chloride and Cesium Chloride. *Bull. Chem. Soc. Jpn.* **1979**, *52*, 2755−2759.

(5) Yamagami, M.; Yamaguchi, T.; Wakita, H.; Misawa, M. Pulsed Neutron Diffraction Study on Lithium (I) Hydration in Supercooled Aqueous Chloride Solutions. *J. Chem. Phys.* **1994**, *100*, 3122−3126.

(6) Leberman, R.; Soper, A. K. Effect of High Salt Concentrations on Water Structure. *Nature* **1995**, *378*, 364−366.

(7) Soper, A. K.; Weckström, K. Ion Solvation and Water Structure in Potassium Halide Aqueous Solutions. *Biophys. Chem.* **2006**, *124*, 180−191.

(8) Mancinelli, R.; Botti, A.; Bruni, F.; Ricci, M. A.; Soper, A. K. Hydration of Sodium, Potassium, and Chloride Ions in Solution and the Concept of Structure Maker/Breaker. *J. Phys. Chem. B* **2007**, *111*, 13570−13577.

(9) Bouazizi, S.; Hammami, F.; Nasr, S.; Bellissent-Funel, M. C. Neutron Scattering Experiments on Aqueous Sodium Chloride Solutions and Heavy Water. Comparison to Molecular Dynamics and X-ray Results. *J. Mol. Struct.* **2008**, *892*, 47−52.

(10) Bouazizi, S.; Nasr, S.; Jaîdane, N.; Bellissent-Funel, M. C. Local Order in Aqueous NaCl Solutions and Pure Water: X-ray Scattering and Molecular Dynamics Simulations Study. *J. Phys. Chem. B* **2006**, *110*, 23515−23523.

(11) Bouazizi, S.; Nasr, S. Local Order in Aqueous Lithium Chloride Solutions as Studied by X-ray Scattering and Molecular Dynamics Simulations. *J. Mol. Struct.* **2007**, *837*, 206−213.

(12) Bouazizi, S.; Nasr, S. Structural Investigations of High Concentrated Aqueous LiCl Solutions: X-ray Scattering and MD Simulations Approach. *J. Mol. Struct.* **2008**, *875*, 121−129.

(13) Mähler, J.; Persson, I. A Study of the Hydration of the Alkali Metal Ions in Aqueous Solution. *Inorg. Chem.* **2012**, *51*, 425−438.

(14) Glezakou, V. A.; Chen, Y. S.; Fulton, J. L.; Schenter, G. K.; Dang, L. X. Electronic Structure, Statistical Mechanical Simulations, and EXAFS Spectroscopy of Aqueous Potassium. *Theor. Chem. Acc.* **2006**, *115*, 86−99.

(15) Antalek, M.; Pace, E.; Hedman, B.; Hodgson, K. O.; Chillemi, G.; Benfatto, M.; Sarangi, R.; Frank, P. Solvation Structure of the Halides from X-ray Absorption Spectroscopy. *J. Chem. Phys.* **2016**, *145*, 044318.

(16) Megyes, T.; Bálint, S.; Grósz, T.; Radnai, T.; Bakó, I.; Sipos, P. The Structure of Aqueous Sodium Hydroxide Solutions: A Combined Solution X-ray Diffraction and Simulation Study. *J. Chem. Phys.* **2008**, *128*, 044501.

(17) Winter, B.; Weber, R.; Hertel, I. V.; Faubel, M.; Jungwirth, P.; Brown, E. C.; Bradforth, S. E. Electron Binding Energies of Aqueous Alkali and Halide Ions: EUV Photoelectron Spectroscopy of Liquid Solutions and Combined Ab Initio and Molecular Dynamics Calculations. *J. Am. Chem. Soc.* **2005**, *127*, 7203−7214.

(18) Yin, Z.; Rajkovic, I.; Kubicek, K.; Quevedo, W.; Pietzsch, A.; Wernet, P.; Föhlisch, A.; Techert, S. Probing the Hofmeister Effect with Ultrafast Core-Hole Spectroscopy. *J. Phys. Chem. B* **2014**, *118*, 9398−9403.

(19) Jeyachandran, Y. L.; Meyer, F.; Benkert, A.; Bär, M.; Blum, M.; Yang, W.; Reinert, F.; Heske, C.; Weinhardt, L.; Zharnikov, M. Investigation of the Ionic Hydration in Aqueous Salt Solutions by Soft X-ray Emission Spectroscopy. *J. Phys. Chem. B* **2016**, *120*, 7687−7695.

(20) Yin, Z.; Inhester, L.; Veedu, S. T.; Quevedo, W.; Pietzsch, A.; Wernet, P.; Groenhof, G.; Föhlisch, A.; Grubmüller, H.; Techert, S. Cationic and Anionic Impact on the Electronic Structure of Liquid Water. *J. Phys. Chem. Lett.* **2017**, *8*, 3759−3764.

(21) Tóth, G. *Ab Initio* Pair Potential Parameter Set for the Interaction of a Rigid and a Flexible Water Model and the Complete Series of the Halides and Alkali Cations. *J. Chem. Phys.* **1996**, *105*, 5518−5524.

(22) Tongraar, A.; Liedl, K. R.; Rode, B. M. The Hydration Shell Structure of Li^+ Investigated by Born-Oppenheimer Ab Initio QM/MM Dynamics. *Chem. Phys. Lett.* **1998**, *286*, 56−64.

(23) White, J. A.; Schwegler, E.; Galli, G.; Gygi, F. The Solvation of Na^+ in Water: First-Principles Simulations. *J. Chem. Phys.* **2000**, *113*, 4668−4673.

(24) Egorov, A. V.; Komolkin, A. V.; Chizhik, V. I.; Yushmanov, P. V.; Lyubartsev, A. P.; Laaksonen, A. Temperature and Concentration Effects on Li^+-Ion Hydration. A Molecular Dynamics Simulation Study. *J. Phys. Chem. B* **2003**, *107*, 3234−3242.

(25) Spångberg, D.; Hermansson, K. Many-Body Potentials for Aqueous Li^+, Na^+, Mg^{2+}, and Al^{3+}: Comparison of Effective Three-Body Potentials and Polarizable Models. *J. Chem. Phys.* **2004**, *120*, 4829−4843.

DOI: 10.1021/acs.jpcb.7b09789
J. Phys. Chem. B 2017, 121, 10957−10964

(26) Chowdhuri, S.; Chandra, A. Dynamics of Halide Ion-Water Hydrogen Bonds in Aqueous Solutions: Dependence on Ion Size and Temperature. *J. Phys. Chem. B* **2006**, *110*, 9674−9680.
(27) Guàrdia, E.; Laria, D.; Martí, J. Hydrogen Bond Structure and Dynamics in Aqueous Electrolytes at Ambient and Supercritical Conditions. *J. Phys. Chem. B* **2006**, *110*, 6332−6338.
(28) Thomas, A. S.; Elcock, A. H. Molecular Dynamics Simulations of Hydrophobic Associations in Aqueous Salt Solutions Indicate a Connection between Water Hydrogen Bonding and the Hofmeister Effect. *J. Am. Chem. Soc.* **2007**, *129*, 14887−14898.
(29) Liu, Y.; Lu, H. G.; Wu, Y. B.; Hu, T. P.; Li, Q. L. Hydration and Coordination of K^+ Solvation in Water from *Ab Initio* Molecular-Dynamics Simulation. *J. Chem. Phys.* **2010**, *132*, 124503.
(30) Bankura, A.; Carnevale, V.; Klein, M. L. Hydration Structure of Salt Solutions from *Ab Initio* Molecular Dynamics. *J. Chem. Phys.* **2013**, *138*, 014501.
(31) Galamba, N. On the Effects of Temperature, Pressure, and Dissolved Salts on the Hydrogen-Bond Network of Water. *J. Phys. Chem. B* **2013**, *117*, 589−601.
(32) Sripa, P.; Tongraar, A.; Kerdcharoen, T. "Structure-Making" Ability of Na^+ in Dilute Aqueous Solution: An ONIOM-XS MD Simulation Study. *J. Phys. Chem. A* **2013**, *117*, 1826−1833.
(33) Gaiduk, A. P.; Zhang, C.; Gygi, F.; Galli, G. Structural and Electronic Properties of Aqueous NaCl Solutions from Ab Initio Molecular Dynamics Simulations with Hybrid Density Functionals. *Chem. Phys. Lett.* **2014**, *604*, 89−96.
(34) Xu, J. J.; Yi, H. B.; Li, H. J.; Chen, Y. Ionic Solvation and Association in LiCl Aqueous Solution: A Density Functional Theory, Polarised Continuum Model and Molecular Dynamics Investigation. *Mol. Phys.* **2014**, *112*, 1710−1723.
(35) Aziz, E. F.; Zimina, A.; Freiwald, M.; Eisebitt, S.; Eberhardt, W. Molecular and Electronic Structure in NaCl Electrolytes of Varying Concentration: Identification of Spectral Fingerprints. *J. Chem. Phys.* **2006**, *124*, 114502.
(36) Wachter, W.; Fernandez, Š.; Buchner, R.; Hefter, G. Ion Association and Hydration in Aqueous Solutions of LiCl and Li_2SO_4 by Dielectric Spectroscopy. *J. Phys. Chem. B* **2007**, *111*, 9010−9017.
(37) Rudolph, W.; Brooker, M. H.; Pye, C. C. Hydration of Lithium Ion in Aqueous Solution. *J. Phys. Chem.* **1995**, *99*, 3793−3797.
(38) Li, R. H.; Jiang, Z. P.; Chen, F. G.; Yang, H. W.; Guan, Y. T. Hydrogen Bonded Structure of Water and Aqueous Solutions of Sodium Halides: A Raman Spectroscopic Study. *J. Mol. Struct.* **2004**, *707*, 83−88.
(39) Smith, J. D.; Saykally, R. J.; Geissler, P. L. The Effects of Dissolved Halide Anions on Hydrogen Bonding in Liquid Water. *J. Am. Chem. Soc.* **2007**, *129*, 13847−13856.
(40) Bergmann, U.; Glatzel, P.; Cramer, S. P. Bulk-Sensitive XAS Characterization of Light Elements: From X-ray Raman Scattering to X-ray Raman Spectroscopy. *Microchem. J.* **2002**, *71*, 221−230.
(41) Cavalleri, M.; Ogasawara, H.; Pettersson, L. G. M.; Nilsson, A. The Interpretation of X-ray Absorption Spectra of Water and Ice. *Chem. Phys. Lett.* **2002**, *364*, 363−370.
(42) Myneni, S.; Luo, Y.; Näslund, L. Å.; Cavalleri, M.; Ojamäe, L.; Ogasawara, H.; Pelmenschikov, A.; Wernet, P.; Väterlein, P.; Heske, C.; et al. Spectroscopic Probing of Local Hydrogen-Bonding Structures in Liquid Water. *J. Phys.: Condens. Matter* **2002**, *14*, L213−L219.
(43) Smith, J. D.; Cappa, C. D.; Wilson, K. R.; Messer, B. M.; Cohen, R. C.; Saykally, R. J. Energetics of Hydrogen Bond Network Rearrangements in Liquid Water. *Science* **2004**, *306*, 851−853.
(44) Wernet, P.; Nordlund, D.; Bergmann, U.; Cavalleri, M.; Odelius, M.; Ogasawara, H.; Näslund, L. Å.; Hirsch, T. K.; Ojamäe, L.; Glatzel, P.; et al. The Structure of the First Coordination Shell in Liquid Water. *Science* **2004**, *304*, 995−999.
(45) Näslund, L. Å.; Lüning, J.; Ufuktepe, Y.; Ogasawara, H.; Wernet, P.; Bergmann, U.; Pettersson, L. G. M.; Nilsson, A. X-ray Absorption Spectroscopy Measurements of Liquid Water. *J. Phys. Chem. B* **2005**, *109*, 13835−13839.
(46) Odelius, M.; Cavalleri, M.; Nilsson, A.; Pettersson, L. G. M. X-ray Absorption Spectrum of Liquid Water from Molecular Dynamics Simulations: Asymmetric Model. *Phys. Rev. B: Condens. Matter Mater. Phys.* **2006**, *73*, 024205.
(47) Huang, C.; Wikfeldt, K. T.; Tokushima, T.; Nordlund, D.; Harada, Y.; Bergmann, U.; Niebuhr, M.; Weiss, T. M.; Horikawa, Y.; Leetmaa, M.; et al. The Inhomogeneous Structure of Water at Ambient Conditions. *Proc. Natl. Acad. Sci. U. S. A.* **2009**, *106*, 15214−15218.
(48) Nagasaka, M.; Hatsui, T.; Horigome, T.; Hamamura, Y.; Kosugi, N. Development of a Liquid Flow Cell to Measure Soft X-ray Absorption in Transmission Mode: A Test for Liquid Water. *J. Electron Spectrosc. Relat. Phenom.* **2010**, *177*, 130−134.
(49) Pylkkänen, T.; Sakko, A.; Hakala, M.; Hämäläinen, K.; Monaco, G.; Huotari, S. Temperature Dependence of the near-Edge Spectrum of Water. *J. Phys. Chem. B* **2011**, *115*, 14544−14550.
(50) Schreck, S.; Gavrila, G.; Weniger, C.; Wernet, P. A Sample Holder for Soft X-ray Absorption Spectroscopy of Liquids in Transmission Mode. *Rev. Sci. Instrum.* **2011**, *82*, 103101.
(51) Meibohm, J.; Schreck, S.; Wernet, P. Temperature Dependent Soft X-ray Absorption Spectroscopy of Liquids. *Rev. Sci. Instrum.* **2014**, *85*, 103102.
(52) Sellberg, J. A.; Kaya, S.; Segtnan, V. H.; Chen, C.; Tyliszczak, T.; Ogasawara, H.; Nordlund, D.; Pettersson, L. G. M.; Nilsson, A. Comparison of X-ray Absorption Spectra between Water and Ice: New Ice Data with Low Pre-Edge Absorption Cross-Section. *J. Chem. Phys.* **2014**, *141*, 034507.
(53) Näslund, L. Å.; Edwards, D. C.; Wernet, P.; Bergmann, U.; Ogasawara, H.; Pettersson, L. G. M.; Myneni, S.; Nilsson, A. X-ray Absorption Spectroscopy Study of the Hydrogen Bond Network in the Bulk Water of Aqueous Solutions. *J. Phys. Chem. A* **2005**, *109*, 5995−6002.
(54) Cappa, C. D.; Smith, J. D.; Messer, B. M.; Cohen, R. C.; Saykally, R. J. The Electronic Structure of the Hydrated Proton: A Comparative X-ray Absorption Study of Aqueous HCl and NaCl Solutions. *J. Phys. Chem. B* **2006**, *110*, 1166−1171.
(55) Cappa, C. D.; Smith, J. D.; Messer, B. M.; Cohen, R. C.; Saykally, R. J. Effects of Cations on the Hydrogen Bond Network of Liquid Water: New Results from X-ray Absorption Spectroscopy of Liquid Microjets. *J. Phys. Chem. B* **2006**, *110*, 5301−5309.
(56) Schwartz, C. P.; Uejio, J. S.; Duffin, A. M.; Drisdell, W. S.; Smith, J. D.; Saykally, R. J. Soft X-ray Absorption Spectra of Aqueous Salt Solutions with Highly Charged Cations in Liquid Microjets. *Chem. Phys. Lett.* **2010**, *493*, 94−96.
(57) Waluyo, I.; Huang, C.; Nordlund, D.; Weiss, T. M.; Pettersson, L. G. M.; Nilsson, A. Increased Fraction of Low-Density Structures in Aqueous Solutions of Fluoride. *J. Chem. Phys.* **2011**, *134*, 224507.
(58) Juurinen, I.; Pylkkänen, T.; Ruotsalainen, K. O.; Sahle, C. J.; Monaco, G.; Hämäläinen, K.; Huotari, S.; Hakala, M. Saturation Behavior in X-ray Raman Scattering Spectra of Aqueous LiCl. *J. Phys. Chem. B* **2013**, *117*, 16506−16511.
(59) Waluyo, I.; Nordlund, D.; Bergmann, U.; Schlesinger, D.; Pettersson, L. G. M.; Nilsson, A. A Different View of Structure-Making and Structure-Breaking in Alkali Halide Aqueous Solutions through X-ray Absorption Spectroscopy. *J. Chem. Phys.* **2014**, *140*, 244506.
(60) Nagasaka, M.; Yuzawa, H.; Horigome, T.; Kosugi, N. Reliable Absorbance Measurement of Liquid Samples in Soft X-ray Absorption Spectroscopy in Transmission Mode. *J. Electron Spectrosc. Relat. Phenom.* **2017**, DOI: 10.1016/j.elspec.2017.05.004.
(61) Soper, A. K. The Radial Distribution Functions of Water and Ice from 220 to 673 K and at Pressures up to 400 MPa. *Chem. Phys.* **2000**, *258*, 121−137.
(62) Modig, K.; Pfrommer, B. G.; Halle, B. Temperature-Dependent Hydrogen-Bond Geometry in Liquid Water. *Phys. Rev. Lett.* **2003**, *90*, 075502.
(63) Hakala, M.; Nygård, K.; Manninen, S.; Pettersson, L. G. M.; Hämäläinen, K. Intra- and Intermolecular Effects in the Compton Profile of Water. *Phys. Rev. B: Condens. Matter Mater. Phys.* **2006**, *73*, 035432.

DOI: 10.1021/acs.jpcb.7b09789
J. Phys. Chem. B 2017, 121, 10957−10964

(64) Nygård, K.; Hakala, M.; Pylkkänen, T.; Manninen, S.; Buslaps, T.; Itou, M.; Andrejczuk, A.; Sakurai, Y.; Odelius, M.; Hämäläinen, K. Isotope Quantum Effects in the Electron Momentum Density of Water. *J. Chem. Phys.* **2007**, *126*, 154508.
(65) Smith, J. D.; Cappa, C. D.; Wilson, K. R.; Cohen, R. C.; Geissler, P. L.; Saykally, R. J. Unified Description of Temperature-Dependent Hydrogen-Bond Rearrangements in Liquid Water. *Proc. Natl. Acad. Sci. U. S. A.* **2005**, *102*, 14171−14174.
(66) Auer, B. M.; Skinner, J. L. IR and Raman Spectra of Liquid Water: Theory and Interpretation. *J. Chem. Phys.* **2008**, *128*, 224511.
(67) Kraemer, D.; Cowan, M. L.; Paarmann, A.; Huse, N.; Nibbering, E. T. J.; Elsaesser, T.; Miller, R. J. D. Temperature Dependence of the Two-Dimensional Infrared Spectrum of Liquid H_2O. *Proc. Natl. Acad. Sci. U. S. A.* **2008**, *105*, 437−442.
(68) Paolantoni, M.; Lago, N. F.; Albertí, M.; Laganà, A. Tetrahedral Ordering in Water: Raman Profiles and Their Temperature Dependence. *J. Phys. Chem. A* **2009**, *113*, 15100−15105.
(69) Errington, J. R.; Debenedetti, P. G. Relationship between Structural Order and the Anomalies of Liquid Water. *Nature* **2001**, *409*, 318−321.
(70) Yan, Z. Y.; Buldyrev, S. V.; Kumar, P.; Giovambattista, N.; Debenedetti, P. G.; Stanley, H. E. Structure of the First- and Second-Neighbor Shells of Simulated Water: Quantitative Relation to Translational and Orientational Order. *Phys. Rev. E* **2007**, *76*, 051201.
(71) Nagasaka, M.; Mochizuki, K.; Leloup, V.; Kosugi, N. Local Structures of Methanol-Water Binary Solutions Studied by Soft X-ray Absorption Spectroscopy. *J. Phys. Chem. B* **2014**, *118*, 4388−4396.
(72) Nagasaka, M.; Yuzawa, H.; Kosugi, N. Development and Application of in situ/Operando Soft X-ray Transmission Cells to Aqueous Solutions and Catalytic and Electrochemical Reactions. *J. Electron Spectrosc. Relat. Phenom.* **2015**, *200*, 293−310.
(73) Hatsui, T.; Shigemasa, E.; Kosugi, N. Design of a Transmission Grating Spectrometer and an Undulator Beamline for Soft X-ray Emission Studies. *AIP Conf. Proc.* **2003**, *705*, 921−924.
(74) Coreno, M.; de Simone, M.; Prince, K. C.; Richter, R.; Vondráček, M.; Avaldi, L.; Camilloni, R. Vibrationally Resolved Oxygen K → Π* Spectra of O_2 and CO. *Chem. Phys. Lett.* **1999**, *306*, 269−274.
(75) Hess, B.; Kutzner, C.; van der Spoel, D.; Lindahl, E. GROMACS 4: Algorithms for Highly Efficient, Load-Balanced, and Scalable Molecular Simulation. *J. Chem. Theory Comput.* **2008**, *4*, 435−447.
(76) Abraham, M. J.; Murtola, T.; Schulz, R.; Páll, S.; Smith, J. C.; Hess, B.; Lindahl, E. GROMACS: High Performance Molecular Simulations through Multi-Level Parallelism from Laptops to Supercomputers. *SoftwareX* **2015**, *1*−*2*, 19−25.
(77) Jorgensen, W. L.; Tirado-Rives, J. Potential Energy Functions for Atomic-Level Simulations of Water and Organic and Biomolecular Systems. *Proc. Natl. Acad. Sci. U. S. A.* **2005**, *102*, 6665−6670.
(78) Caleman, C.; van Maaren, P. J.; Hong, M. Y.; Hub, J. S.; Costa, L. T.; van der Spoel, D. Force Field Benchmark of Organic Liquids: Density, Enthalpy of Vaporization, Heat Capacities, Surface Tension, Isothermal Compressibility, Volumetric Expansion Coefficient, and Dielectric Constant. *J. Chem. Theory Comput.* **2012**, *8*, 61−74.
(79) Mahoney, M. W.; Jorgensen, W. L. A Five-Site Model for Liquid Water and the Reproduction of the Density Anomaly by Rigid, Nonpolarizable Potential Functions. *J. Chem. Phys.* **2000**, *112*, 8910−8922.
(80) Nosé, S. A Unified Formulation of the Constant Temperature Molecular Dynamics Methods. *J. Chem. Phys.* **1984**, *81*, 511−519.
(81) Hoover, W. G. Canonical Dynamics: Equilibrium Phase-Space Distributions. *Phys. Rev. A: At., Mol., Opt. Phys.* **1985**, *31*, 1695−1697.
(82) Parrinello, M.; Rahman, A. Polymorphic Transitions in Single Crystals: A New Molecular Dynamics Method. *J. Appl. Phys.* **1981**, *52*, 7182−7190.
(83) Darden, T.; York, D.; Pedersen, L. Particle Mesh Ewald: An $N\cdot\log(N)$ Method for Ewald Sums in Large Systems. *J. Chem. Phys.* **1993**, *98*, 10089−10092.

DOI: 10.1021/acs.jpcb.7b09789
J. Phys. Chem. B 2017, 121, 10957−10964